Engineering Science and Technology, an International Journal 35 (2022) 101264

HOSTED BY

Contents lists available at ScienceDirect

Engineering Science and Technology, an International Journal

journal homepage: www.elsevier.com/locate/jestch

Fast and optimal tuning of fractional order PID controller for AVR system based on memorizable-smoothed functional algorithm

RenHao Mok *, Mohd Ashraf Ahmad *

Faculty of Electrical and Electronics Engineering Technology, University Malaysia Pahang, Pekan, Malaysia

ARTICLE INFO

Article history:
Received 22 March 2022
Revised 4 August 2022
Accepted 24 September 2022
Available online 28 October 2022

Keywords:
Smoothed Functional Algorithm
Automatic voltage regulator
Fractional PID controller
Gradient based
Optimization

ABSTRACT

Voltage regulation in automatic voltage regulator (AVR) system has been one of the most challenging engineering problem due to the uncertain load condition. Therefore, the control of AVR system by using PID based controller is one of the essential approach to maintain the performance of the AVR system. Subsequently, the application of FOPID controller in AVR system is gaining more attention recently. This is because the FOPID has additional control parameters at the derivative and integral parts than the PID controller, which has the advantage to improve the output response of AVR system while retaining the robustness and simple construction as the PID controller. Nevertheless, many existing optimization tools for tuning the FOPID controller, which are based on multi-agent based optimization, require large number of function evaluation in their algorithm that could lead to high computational burden. Therefore, this study proposes a modified smoothed function algorithm (MSFA) based method to tune the FOPID controller of AVR system since it requires fewer number of function evaluation per iteration. Moreover, the proposed MSFA based method also can solve the unstable convergence issue in the original smoothed function algorithm (SFA), thus able to provide better convergence accuracy. The simulations of step response analysis, Bode plot analysis, trajectory tracking analysis, disturbance rejection analysis, and parameter variation analysis are conducted to evaluate the effectiveness of the proposed MSFA-FOPID controller of AVR system. Consequently, the results obtained from the simulations revealed that the proposed method is highly effective and significantly improved as compared to the other existing FOPID controllers.

1. Introduction

The application of Automatic Voltage Regular (AVR) system has become more ubiquitous in order to improve the power quality of electrical power system. In particular, the uncertain load condition in electrical power system could degrade the power quality by causing the terminal voltage in electrical power system to vary [1]. Therefore, voltage regulation by using the AVR system is one of the effective approaches to improve the power quality in electrical power system. Specifically, the AVR system is utilized to produce near constant voltage over a wide range of load conditions. In general, a conventional AVR system is an uncontrolled closed-loop system consists of several components, which includes the amplifier, exciter, generator, and sensor [2]. The working principle of the conventional AVR system is that the terminal voltage produced in the generator is monitored by the sensor, then the amplifier sets the amount of current in the exciter to produce just enough magnetic field for power production in the generator based on the error between the monitored generator's terminal voltage value and the reference input voltage. As a result, the generator is able to provide near constant terminal voltage for a wide range of load condition. However, despite the conventional AVR system may offer stable voltage regulation without the use of a controller, it is still inefficient and insufficiently robust since the terminal voltage fluctuations still exist and requires longer time to achieve steady state [3]. Eventually, the development of AVR system based on closed-loop control structure was intensively conducted by many researchers in the attempt to resolve these issues.

There are various control techniques had been proposed in a few decades ago in the attempt to control the terminal voltage of AVR system. For example, PID controller [4–15], Sigmoid-PID controller [16,29,30], Fractional-order PID (FOPID) controller [17–22], single-neuron PID [23–25], Fuzzy-PID [26–28], sliding mode controller [31], Fuzzy Logic controller [20], fractional high-order differential feedback controller [32], are some of the proposed control techniques for application in AVR system. Nevertheless,

* Corresponding authors.
E-mail addresses: mokrenhao@gmail.com (R. Mok), mashraf@ump.edu.my (M.A. Ahmad).

https://doi.org/10.1016/j.jestch.2022.101264
2215-0986/

the variants of PID controller have attracted the greatest attention from the researchers and industry due to their robustness, easy to understand, and uncomplicated control structure. In particular, the newer FOPID controller is getting more popular over the conventional PID controller since the FOPID controller can provide better performance in terms of rise time, settling time, overshoot, and steady state error while retaining the similar simple structure as the conventional PID controller [33]. Unlike the conventional PID controller which only consists of three control parameters, specifically the gain of proportional K_P, the gain of integral K_I, and the gain of derivative K_D, the newer FOPID controller introduces two more fractional exponential terms of integral λ and derivative μ. Hence, by having five control parameters, the FOPID controller can deliver more flexible design in various engineering field such as the control of generator's terminal voltage in AVR system. However, before the FOPID controller can fully utilize its capabilities in controlling the AVR system, it must first be tuned. As a result, the tuning of FOPID controller can be more challenging since it contains more control parameters than the conventional PID controller. Thus, in order to acquire the optimal FOPID controller parameters, it is crucial to choose an appropriate optimization method.

A number of optimization methods based on stochastic approach have been widely used to tune the FOPID controller in obtaining the optimum control parameters. In particular, the optimization method such as the Chaotic Ant Swarm (CAS) [34], Non-dominated Sorting Genetic Algorithm (NSGA II) [35], Particle Swarm Optimization (PSO) [36], Simulated Annealing Algorithm (SA) [13], and Sine Cosine Algorithm (SCA) [37] based methods have shown to be efficient in tuning the FOPID controller of the AVR system. Although these optimization based methods can produce an optimum FOPID controllers, they require heavy computational load during the tuning process. This is because the computation times per iteration are proportional to the number of agents, thus increases the computational effort in order to obtain the optimum FOPID controller. Moreover, the additional control parameters in the FOPID controller also exacerbating the computational load. Therefore, the multi-agent optimization based method maybe not a practical choice and it is necessary to synthesize a tuning strategy that requires less computational times. Meanwhile, a Smoothed Functional Algorithm (SFA), which is in the class of gradient-based optimization method, is promising optimization tool from the perspective of having low computational effort in tuning the FOPID controller. This is because this algorithm only requires two objective function evaluations per iteration in performing the gradient approximation. Moreover, the SFA also is known to be effective in solving various optimization problems even for large number of tuning parameters [38–40]. Hence, it is worth to investigate the capability of the SFA based method in tuning the FOPID controller of AVR system.

The original SFA based method is based on stochastic search using smoothed functional (SF) scheme, whereby the gradient approximation is computed based on convolution approach [38]. On the other hand, the two-timescale of the SF scheme proposed in Bhatnagar and Borkar [41] can provide a simpler solution. Here, the gradient approximation is estimated by using two simultaneous objective function evaluations. Here, the evaluations of objective function are conducted based on two different design variable vectors that are perturbed randomly around its current values. In this study, the two-timescale SF scheme is chosen, and it is normally known as the SFA based method. Nevertheless, the application of SFA based method in solving engineering problem remains challenging. This is because the SFA based method is unable to provide stable solution due to its update vector tends to be unpredictable and cause divergence [42]. On the other hand, one of the features in the Random Search (RS) based method [43,44] known as the memorizable function that has the capability to store the best solution is helpful to stabilize the output even though the update vector has become unpredictable. Furthermore, the memorizable function is also capable to improve the convergence accuracy of optimization method as the evaluation of the update vector is always starting from the best solution. Thus, this study is motivated to adopt the memorizable function in the SFA based method to tune the FOPID in AVR system.

In overall, this paper presents a new approach to tune the FOPID controller in AVR system using the proposed SFA based method with memorizable function (MSFA). In particular, a new MSFA-FOPID controller is developed, whereby the MSFA based method is used to optimize the control parameters (K_P, K_I, K_D, λ, μ) in the FOPID controller. Then, the MSFA-FOPID controller is implemented in an AVR system to provide optimum voltage regulation control. Eventually, several study cases are conducted to investigate and compare the performance of the MSFA-FOPID controller with the other existing optimization based FOPID controllers, which are SCA-FOPID [37], SA-FOPID [13], CAS-FOPID [34], PSO-FOPID [36], and NSGA II-FOPID [35]. Firstly, step response analysis is conducted to examine the control performance of the optimum FOPID controller obtained by the MSFA based method. Subsequently, the control performance is evaluated in terms of overshoot, settling time, rise time, and steady state error. Meanwhile, the Function of Demerit (FOD) as introduced in [11] is also included in this analysis to compare the overall performance of the optimization based FOPID controllers. Moreover, numbers of function evaluation (NFE) is introduced in this analysis to compare the computational load of the optimization based FOPID controllers, where the NFE is defined as the total number of objective function evaluations required for an optimization based method in obtaining the optimum FOPID controller throughout all iterations. Then, the improvement of the new MSFA over the SFA based method is highlighted in statistical analysis of FOD. Furthermore, the stability of the optimization based FOPID AVR systems are analyzed in terms of phase margin, delay margin, and peak gain in the Bode plot analysis. The robustness of the FOPID AVR systems is also tested by conducting trajectory tracking, disturbance rejection, and parameter variation analyses. Here, the Integral-Absolute-Error (IAE), Integral-Square-Error (ISE), Integral-Time-Absolute-Error (ITAE), and Integral-Time-Square-Error (ITSE) are used for the robustness evaluation. Thus, the contributions of this study are highlighted as follows:

A new MSFA based method is developed by implementing a memorizable function in the SFA based method. Specifically, the memorizable function in the MSFA based method is used to store the best solution obtained from every iteration. The benefit of this implementation can help to avoid the divergence problem in SFA based method as the update vector in the MSFA based method is always computed from the best solution.

The new MSFA based method can effectively tune the FOPID controller of AVR system by requiring fewer NFE. Therefore, the proposed MSFA can solve the high computational load issue in most of the multi-agent based optimization methods, thus it will be more practical for real-time tuning control of AVR system.

A new reference signal consists of step and ramp signals is introduced for performance evaluation of the proposed MSFA-FOPID controller in both trajectory tracking and disturbance rejection analyses. As a result, such a reference signal gives a better indicator of the proposed method's efficiency level in comparison to other existing FOPID controllers.

The level of disturbance signal used in this study is more significant as compared with other previous studies as the peak to peak amplitude of the disturbance signal is 50% of the reference input signal. Meanwhile, the disturbance signal rejection analysis is conducted along with trajectory tracking study case to reflect the real application of AVR system.

The following is the outline of this paper. Section 1 introduces the background of the tunning of FOPID controller in AVR system by using the proposed MSFA based method. Moreover, the formulated problem concerning the FOPID AVR system is described in Section 2. Then, Section 3 explains the methodology of MSFA. This is followed by the discussion of the obtained results and comparisons on the tuning of FOPID controller in AVR system using MSFA based method and the other counterparts are discussed in Section 4 through several study cases. Lastly, Section 5 summarizes the findings of this study.

2. Problem formulation of FOPID AVR system

In this section, the problem formulation of AVR system with FOPID controller (FOPID AVR) is explained. Firstly, the mathematical model of AVR system in terms of several transfer function blocks is described. Then, the construction of the AVR system with FOPID controller is provided. Furthermore, the predefined parameters in the mathematical model of AVR system to ensure the stability of the system are discussed. Lastly, the problem formulation of the FOPID AVR system is expressed in the end of this section.

Fig. 1 shows the overview of AVR system. In general, amplifier, exciter, sensor, and generator are the four main components in the AVR system. During power generation, the unregulated generator's terminal voltage could be fluctuating as a result of inconsistence load, which will significantly degrade the power quality. Therefore, a close loop system such as AVR system is essential to retain the highest power quality. In the AVR system, the generator's terminal voltage is monitored by the voltage feedback sensor. Then, the amplifier amplifies the voltage error between the feedback voltage and referenced voltage. If the voltage error rises positively, the exciter increases the excitation to increase the voltage gain, and vice versa. Hence, the terminal voltage of the generator is being regulated and retained the power quality.

According to the illustration in Fig. 1, the construction of AVR system consists of four major components known as amplifier, exciter, sensor, and generator. Whereby, the transfer function of amplifier, exciter, sensor, and generator can be presented in the following equations:

$$H_A(s) = \frac{K_A}{1 + sT_A}, \tag{1}$$

$$H_E(s) = \frac{K_E}{1 + sT_E}, \tag{2}$$

$$H_G(s) = \frac{K_G}{1 + sT_G}, \tag{3}$$

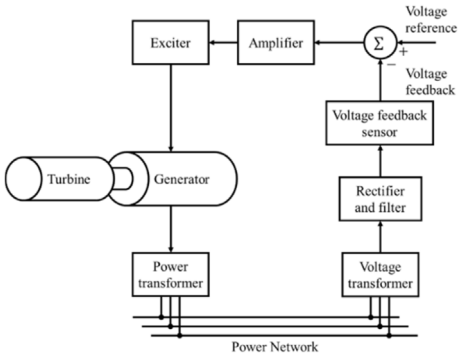

Fig. 1. Overview of AVR system.

$$H_S(s) = \frac{K_S}{1 + sT_S}, \tag{4}$$

respectively. Here, the gains of the amplifier, exciter, generator, and sensor are represented by K_A, K_E, K_G, and K_S, respectively. Meanwhile, T_A, T_E, T_G, and T_S are the time constants for the same components. The transfer function of the FOPID controller, on the other hand, is denoted by

$$K_{FOPID}(s) = K_P + \frac{K_I}{s^{\lambda}} + K_D s^{\mu}, \tag{5}$$

where K_P is the gain of proportional, K_I is the gain of integral, K_D is the gain of derivative, λ is the exponent of integral term, and μ is the exponent of differential term. As a result, the AVR system with FOPID controller can be represented in a closed-loop system control diagram as demonstrated in Fig. 2. Consequently, V_{ref} is the reference input voltage, V_{in} is the feedback voltage, and V_{out} is the output voltage to the power network.

Next, it is appropriate to restrict the value ranges of the components' parameters in the AVR system and the FOPID gains in order to guarantee the system's stability. Whereby, the values are as tabulated in Table 1. Please keep in mind that the value ranges specified are designed to ensure the AVR system is stable, and they are not the optimal settings. Despite the fact that the AVR is stable, the step voltage response of the AVR system in the absence of a controller is extremely oscillatory as shown in Fig. 3.

Furthermore, the performance index proposed in [11] is used to evaluate the performance of the AVR system controlled by the FOPID controller, which is formulated by

$$J(K_P, K_i, K_d, \lambda, \mu) = \left(1 - e^{-\beta}\right)\left(M_p + e_{ss}\right) + e^{-\beta}(t_s - t_r). \tag{6}$$

In this equation, $e_{ss}, M_p, t_r,$ and t_s denote steady-state error, overshoot, rising time, and settling time, respectively. Meanwhile, according to [45], β is a weighting factor such that $0.5 \leq \beta \leq 1.5$ and $\beta = 1.0$ is set in this paper. As a result, the problem can be described as:

Problem 2.1. Based on the given closed-loop system block diagram in

Fig. 2, find the value of FOPID gains K_P, K_i, K_d, λ and μ such that $J(K_P, K_i, K_d, \lambda, \mu)$ is minimized.

3. The standard SFA based method

In this section, the solution to solve Problem 2.1 by using SFA based method is proposed. Firstly, the structure of the standard SFA based method is reviewed. Then, the motivation to propose the MSFA based method in order to overcome the imperfection of the standard SFA based method, such as unstable convergence, is demonstrated. Eventually, the working principal of the proposed MSFA based method to solve the Problem 2.1 is introduced at the end of this section.

3.1. The standard SFA based method

Assume the following optimization problem:

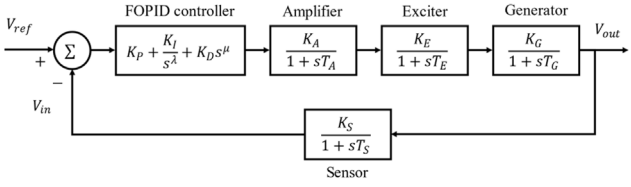

Fig. 2. Closed-loop system block diagram of AVR system with FOPID controller.

Table 1
Parameter ranges of AVR system.

Model	Used values in AVR system
Amplifier	$K_A = 10.00$, $T_A = 0.10$
Exciter	$K_E = 1.00$, $T_E = 0.40$
Generator	$K_G = 1.00$, $T_G = 1.00$
Sensor	$K_S = 1.00$, $T_S = 0.01$

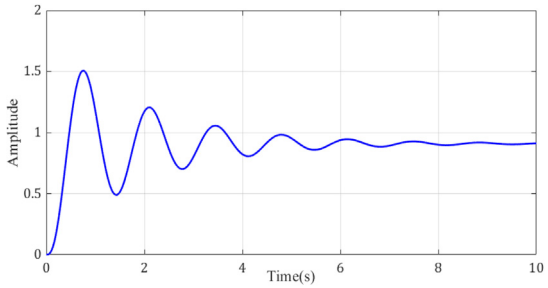

Fig. 3. Output step response of AVR system without any controller.

$$\min_{x \in R^n} h(x), \tag{7}$$

where $x \in R^n$ represent the design variables and $h : R^n \rightarrow R$ typifies an objective function. In order to achieve local optimum $x^* \in R^n$ and $h^* : R^n \rightarrow R$, the designed variable x must be iteratively updated. As a result, the solution is updated using the standard SFA based method as follow:

$$x(k+1) = x(k) - a(k)g(x(k), \Delta(k)), \tag{8}$$

for $k = 1, 2, \cdots, k_{\max}$. For simplicity of the future explanation, let $x_i \in R$ and $x_i^* \in R$ be the i^{th} element of x and x^*, respectively. Subsequently, in (8), $k_{\max}$ is the maximum number of iterations, $x(k) \in R^n$ is the design variable at iteration k, $a(k) \in R^n$ is the dynamic gain of gradient function, $g(x(k), \Delta(k))$ for $a(k+1) < a(k)$ as $k \rightarrow \infty$ and $a(k) > 0$, $\Delta(k)$ is the randomly generated perturbation vector, and $g(x(k), \Delta(k))$ is expressed as

$$g(x(k), \Delta(k)) = \begin{bmatrix} \frac{\Delta_1(k)}{2c(k)}((h(x(k) + c(k)\Delta(k))) - (h(x(k) - c(k)\Delta(k)))) \\ \frac{\Delta_2(k)}{2c(k)}((h(x(k) + c(k)\Delta(k))) - (h(x(k) - c(k)\Delta(k)))) \\ \vdots \\ \frac{\Delta_n(k)}{2c(k)}((h(x(k) + c(k)\Delta(k))) - (h(x(k) - c(k)\Delta(k)))) \end{bmatrix}. \tag{9}$$

Eventually, in (9), $c(k)$ is the dynamic gain of the perturbation vector $\Delta(k)$ such that $c(k+1) < c(k)$ as $k \rightarrow \infty$ and $c(k) > 0$. This method works in a way that $g(x(k), \Delta(k))$ is predicted approximately equal to the gradient of the function h, such as $\delta/\delta x(h(x(k)))$ and therefore (8) stochastically matches the steepest descent. As a result, the convergence is likely to achieve local optimum.

3.2. The MSFA based method

The Smoothed Functional Algorithm based method with memorizable function is proposed in this study to overcome the unstable convergence problem in the Standard SFA based method. There are a number of studies such as [46,42,47] had addressed the similar unstable convergence problem typically found in memoryless stochastic optimization method. This is due to the stochastic and memoryless nature of the standard SFA based method, which causes the solution to vary during optimization that leads to the possibility of the designed parameters, such as $x(k)$, to diverge as $k \rightarrow \infty$. Eventually, two numerical illustrations based on (8) are executed to realize the problem of unstable convergence.

Illustration 1 Stable convergence

For the dimension, $n = 10$, consider the objective function as

$$h(x)h(x-2)^{\top}(x-2) \tag{10}$$

Supposedly, $x_i^* = 2$ for $(i = 1, 2, \cdots, 10)$ are the absolute solution to achieve global minimum point. The convergence curve of $h(x(k))/h(x(0))$ is shown in Fig. 4 with $a(k)h0.5/(k+200)^{0.602}$, $c(k)h0.1/(k+1)^{0.101}$ and randomly initiate $x(0) := [-1.14, -1.58, 2.07, -1.41, -1.26, 3.44, -2.29, -2.22, -1.87, -1.02]^{\top}$. Thus, the algorithm solves the minimization problem.

Illustration 2 Unstable convergence

In this illustration, the dimension is maintained as $n = 10$ and consider a different objective function as

$$h(x)h\left((x-2)^{\top}(x-2)\right)^2 \tag{11}$$

Similarly, $x_i^* = 2$ for $(i = 1, 2, \cdots, 10)$ are remained as the absolute solution to achieve global minimum point. The convergence curve of $h(x(k))/h(x(0))$ is shown in Fig. 5 by retaining the same setting of $a(k)$, $c(k)$, and $x(0)$ as in **Illustration 1**. In this situation, however, $h(x(k))$ is unable to attain the minimal value, indicating that the method is unable to solve the problem.

According to the evidence in Fig. 5, the standard SFA based method is incapable of providing stable convergence for specific situations. As a result, this inspires us to propose an enhanced version of SFA based method by enforcing a memorizable function. By referring back to (8), it is noticeable that the update of the current solution, $x(k+1)$ is always depending on the previous solution, $x(k)$ and the condition of objective function $h(x(k+1)) < h(x(k))$ for minimization problem is not guaranteed in every iteration. Therefore, it is reasonable to create a function that can store the current best solutions, $\bar{x}$ and its corresponding objective function, $\bar{h}$ if the condition $h(x(k+1)) < \bar{h}$ is achieved in any iteration. In this case, the update sequence of the current solution $x(k+1)$ can be always evaluated from the best solution from the previous iteration. Hence, the memorizable solution update based on (8) can now be expressed as:

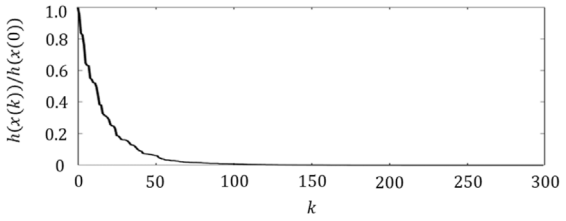

Fig. 4. Convergence curve of $h(x(k))/h(x(0))$ in **Illustration 1**.

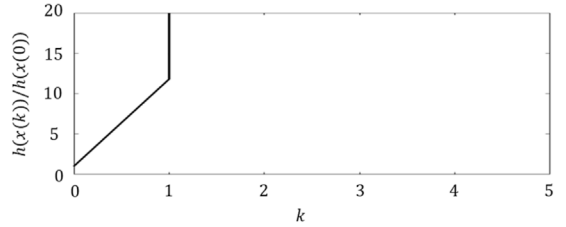

Fig. 5. Convergence curve of $h(x(k))/h(x(0))$ in **Illustration 2**.

$$x(k+1) = \bar{x} - a(k)g\left(\bar{x}, h(k)\right) \tag{12}$$

Thus, the complete procedure of MSFA based method is presented as in Algorithm 3.1.

Algorithm 3.1. Operation of MSFA based method

Set $k = 0$ and determine the termination criterion $k_{\max}$, dynamic gains $a(k)$ and $c(k)$.	
Step (1)	Select the initial design variable $x(0)$ and execute objective function $h(x(0))$. Then, initialize $\bar{x} = x(0)$ and $\bar{h} = h(x(0))$.
Step (2)	Update dynamic gains $a(k)$ and $c(k)$ with the policy as follows: $a(k+1) < a(k)$, $c(k+1) < c(k)$.
Step (3)	Perform the memorizable solution update of SFA based method as in (12) and evaluate objective function, $h(x(k+1))$.
Step (4)	If $h(x(k+1)) < \bar{h}$, then store the optimum solution $\bar{x} = x(k+1)$ and objective function $\bar{h} = h(x(k+1))$. Otherwise, proceed to Step (5).
Step (5)	If $k = k_{\max}$, terminate the algorithm and store the optimum value $x^* = \bar{x}$. Otherwise, set k increment by 1 and repeat Step (2) to Step (5)

Following that, **Illustration 2** is re-executed using Algorithm 3.1 to assess the efficacy of the MSFA based method. The setting for $a(k)$ and $c(k)$ are remained unchanged in this assessment. Finally, Fig. 6 illustrates that the proposed MSFA based method presented in Algorithm 3.1 solved the problem in **Illustration 2** with stable convergence curve. As a result, the implementation of the memorizable function in the SFA based method appears to be promising in terms of resolving an unstable convergence issue in the standard SFA based method.

In practical control systems, a similar divergence issue can easily occur. Specifically, there is high possibility of poles to be located at the right half of the s-plane, which has high risk of the controlled system becoming unstable. As a result, the efficacy of the proposed MSFA will be evaluated in this study by optimizing the FOPID AVR system, especially in finding the optimum K_P, K_i, K_d, λ and μ.

Moreover, in order to verify proposed MSFA in Algorithm 3.1, we also examinate the Algorithm 3.1 with five standard benchmark functions as shown in Table 2. Here, h_1, h_2, h_3, h_4, and h_5 are benchmark functions. Note that h_{min} indicates the global minimum of the benchmark functions. For the standard SFA and the proposed MSFA in Algorithm 3.1, the maximum number of iterations is set at 5000, while the settings of $a(k)$, $c(k)$ and $x(0)$ are retained as in **Illustration 1**.

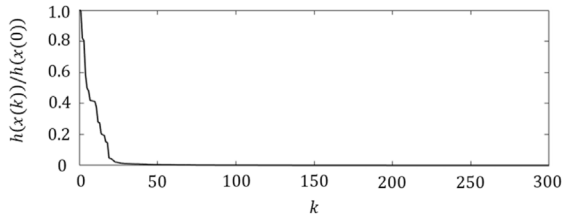

Fig. 6. Convergence curve of $h(x(k))/h(x(0))$ in **Illustration 2** by using the proposed MSFA based method in Algorithm 3.1.

Table 2
Description of benchmark functions.

Function	Dimension	Range	h_{min}
$h_1 = \sum_{i=1}^{n} x_i^2$	10	$[-100, 100]$	0
$h_2 = \sum_{i=1}^{n} \left(\sum_{j-1}^{i} x_j\right)^2$	10	$[-100, 100]$	0
$h_3 = \sum_{i=1}^{n-1} \left[100(x_{i+1} - x_i^2)^2 + (x_i - 1)^2\right]$	10	$[-30, 30]$	0
$h_4 = \sum_{i=1}^{n} (x_i + 0.5)^2$	10	$[-100, 100]$	0
$h_5 = \frac{1}{4000}\sum_{i=1}^{n} x^2 - \prod_{i=1}^{n-1} \cos\left(\frac{x_i}{\sqrt{i}}\right) + 1$	10	$[-600, 600]$	0

For each of the benchmark functions, both the SFA based methods were run 30 times starting from the initial design variable $x(0)$. The statistical results of the mean and standard variation of the objective functions are recorded in Table 3. As observed, the objective function obtained by the proposed MSFA in Algorithm 3.1 are averagely closer to the global optimal for all the benchmark functions. Note that, the objective functions of h_1,

h_2 h_3, and h_4 obtained by the standard SFA are very large, which shows that the standard SFA was unable to solve those problems accurately. Hence, with the statistical result in Table 3, it is justified that the proposed MSFA in Algorithm 3.1 can effectively improve the convergence performance of the standard SFA based method.

3.3. Implementation of the MSFA-FOPID AVR system

Optimization of AVR system with FOPID controller by using the MSFA based method in Algorithm 3.1 is explained in this section. Generally, the MSFA based method is used to tune the K_P, K_i, K_d, λ and μ of the FOPID controller such that J is minimized as shown in Fig. 7.

As a result, the following are the procedures for applying the MSFA in tuning the FOPID of AVR system:

Procedure (1)	Determine the number of maximum iterations $k_{\max}$, which is the termination criterion of the MSFA in Algorithm 3.1. Let $x = [K_P, K_i, K_d, \lambda, \mu]$ and initialize value $x(0)$.
Procedure (2)	Establish the MSFA in Algorithm 3.1 for the objective function J in (6).
Procedure (3)	After $k_{\max}$ iterations of the MSFA in Algorithm 3.1, the optimum design variables $x^* = [K_P^*, K_I^*, K_D^*, \lambda^*, \mu^*]$ is the solution to Problem 2.1.

4. Results and discussions

The effectiveness of the AVR system controlled by the proposed MSFA-FOPID controller is deliberated in this section. As a result, five study cases were considered for this purpose, which are step response, root locus and Bode plot analyses, trajectory tracking, disturbance rejection, and parameter variations of AVR. As for the benchmarking, the proposed MSFA-FOPID controller was compared with the existing FOPID controllers tuned by newly reported modern algorithms of heuristic optimization, which are SCA-FOPID [37], SA-FOPID [13], CAS-FOPID [34], PSO-FOPID [36], and NSGA II [35]. The performance of each method was evaluated according to following criteria:

Table 3
The statistical results of benchmark functions after 30 trials using the SFA based methods.

h	SFA		MSFA	
	Mean	Std.	Mean	Std.
h_1	39.2669	5.6531	3.1827×10^{-5}	7.4634×10^{-6}
h_2	138.8202	48.2736	3.8415×10^{-5}	1.2351×10^{-5}
h_3	4.2053×10^{4}	1.1358×10^{4}	5.0194	0.2586
h_4	0.0095	0.0026	3.3702×10^{-5}	5.9455×10^{-6}
h_5	1.0082	0.0042	4.7332×10^{-6}	8.3972×10^{-7}

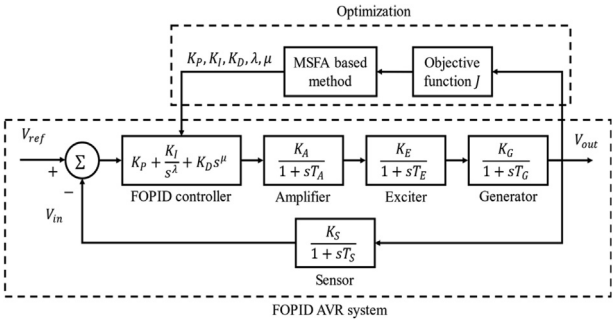

Fig. 7. Construction of MSFA-FOPID AVR system.

The analysis of the time response specifications and the accuracy of FOD, as according to (6).

The computational load in terms of number of function evaluation (NFE) that is used to obtain the optimum controller. In particular, the NFE is defined as the multiplication of $k_{\max}$ and number of evaluated objective functions per iteration.

The statistical analysis of the FOD in terms of its best, mean, worst and standard deviations after 30 trials.

The time and frequency responses analysis in terms of Bode plot, which are used to evaluate the closed-loop system stability.

The trajectory tracking evaluation regarding the Integral-Absolute-Error (IAE), Integral-Square-Error (ISE), Integral-Time-Absolute-Error (ITAE), and Integral-Time-Square-Error (ITSE) even with the existence of disturbance. These performance indicators are mathematically formulated as:

$$\mathrm{IAE} = \int_0^{t_f} |e(t)|dt, \tag{13}$$

$$\mathrm{ISE} = \int_0^{t_f} e^2(t)dt, \tag{14}$$

$$\mathrm{ITAE} = \int_0^{t_f} t|e(t)|dt, \tag{15}$$

$$\mathrm{ITSE} = \int_0^{t_f} te^2(t)dt, \tag{16}$$

where $e(t) = V_{ref}(t) - V_{in}(t)$ and t_f is the final simulation time.

The robustness analysis in terms of the parameter variations in the AVR system.

Furthermore, the simulation of the study has been executed using MATLAB (version: 2018a) in the computer equipped with AMD RYZEN 3700X 3.6GHz processor and 16GB of DDR4 RAM. Meanwhile, in the proposed MSFA and the standard SFA based methods, the dynamic gains are set as $a(k) = 0.2/(k+1)^{0.2}$ and $c(k) = 0.03/(k+1)^{0.03}$. A total of 30 trials were conducted due to the stochastic characteristic of the proposed method is dependent on the generated random numbers. Meanwhile, the termination criterion is set to $k_{\max} = 250$ and $k_{\max} = 375$ for the MSFA and the standard SFA based methods, respectively, to produce an equivalent NFE. Next, the fractional order transfer functions are designed based on 5 $^{\text{th}}$ order Oustaloup with the frequency range of $\omega \in \left[10^{-5}, 10^{5}\right]$ r/s. Moreover, the range of the designed parameters are selected according to the previous studies, where the best K_p, λ, and μ obtained in most of the previous studies [13,37] are smaller than 1.5, and the best K_i, and K_d are smaller than 1.0. Therefore, the upper and lower boundaries of the designed variables x and its initial values $x(0)$ are set as Table 4.

4.1. Step response analysis

This section presents the first case study based on the applied unit step input for FOPID controller of AVR system. Firstly, the FOPID controller parameters are optimized using the proposed MSFA based method using the coefficients and simulation settings stated previously. Then, the time response specification analysis in terms of steady state error, overshoot, rise time and settling time is observed. The analysis is also compared with the standard SFA-FOPID and other existing FOPID controllers. Moreover, the statistical analysis of the FOD in terms of best, mean, worst and standard deviation is also conducted by presenting a comparative assessment between the proposed MSFA and the standard SFA based methods.

The best FOD convergence curve of the proposed MSFA based methods out of 30 individual trials with 750 NFE are shown in Fig. 8. As observed, the FOD has successfully converged from FOD = 0.4361 and achieved the minimum FOD = 0.0209 during NFE = 270. Eventually, the obtained optimum FOPID parameters are shown in Table 5. Note that, the values of λ and μ are fractional or non-integer, which forms a fractional-order PID controller. However, for simulation, it is highly complex to compute the fractional transfer function in the fractional-order PID controller. Therefore, the fractional components in the transfer function are approximated through Oustaloup approximation to form the equivalent integer transfer function with extended number of order to complete the simulation [48–50]. Subsequently, the terminal voltage step responses attained by the proposed MSFA and the other existing FOPID controllers are illustrated in Fig. 9 by using the optimum FOPID controllers' parameters in Table 5. The proposed MSFA-FOPID controller is adequate to produce FOPID controller's param-

Table 4
The FOPID controller parameters and its corresponding design variables with the proposed range and its initial values.

FOPID controller parameters	x	Range	$x(0)$
K_p	x_1	$0.1 < K_p < 1.5$	1.00
K_i	x_2	$0.1 < K_i < 1.0$	1.00
K_d	x_3	$0.1 < K_d < 1.0$	1.00
λ	x_4	$0.1 < \lambda < 1.5$	1.00
μ	x_5	$0.1 < \mu < 1.5$	1.00

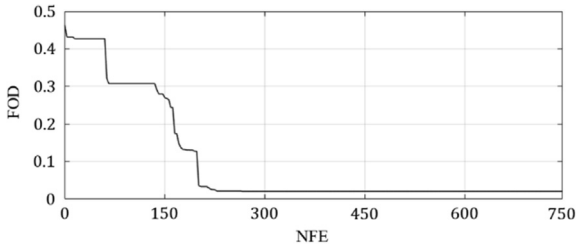

Fig. 8. FOD convergence curve of the MSFA based method.

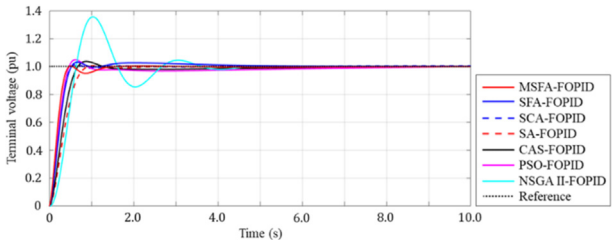

Fig. 9. Step response of AVR system with different controllers.

eters with good control response. It is noticeable that, the response of the MSFA-FOPID controller (red solid line) has quick response in terms of rise time and steady time, while retaining small overshoot and steady state error.

Furthermore, the time response specifications, FOD, and NFE for every optimization based FOPID controllers are recorded in Table 8. Firstly, the time response specification performance is considered and represented by the M_p, t_s, t_r, and e_{ss}. Note that the t_s is defined as the time required to retain 5% of the final value of the unit step input, and the definition of t_r is the time taken in between 10% to 90% of the unit step input's final value. In the comparison of M_p, the proposed MSFA-FOPID is 2.66%, 2.06%, 0.16% and 38.43% smaller than the SFA-FOPID, SCA-FOPID, SA-FOPID and NSGA II-FOPID controllers, while 0.20% and 0.27% larger than the CAS-FOPID and PSO-FOPID controllers, respectively. Hence, it shows that the value of M_p for MSFA-FOPID is slightly comparable with SA-FOPID, CAS-FOPID and PSO-FOPID. Meanwhile, the proposed MSFA-FOPID controller has achieved the fastest t_s with the value of 0.1922 is followed by the SCA-FOPID, SFA-FOPID, CAS-FOPID, SA-FOPID, PSO-FOPID and NSGA II-FOPID controllers. Similarly, the MSFA-FOPID gets the second best t_r after PSO-FOPID with the result of 0.1415 seconds, followed by the SCA-FOPID, SFA-FOPID, CAS-FOPID, SA-FOPID and NSGA II-FOPID controllers. Based on the M_p, t_s, and t_r results, it is justified that the proposed MSFA-FOPID can produce better transient response with much faster unit step terminal voltage tracking and minimum overshoot than other based methods. In terms of the steady state response, the steady state error e_{ss} value is observed, and it is defined as the difference between the value of unit step input and actual output response at t_f, whereby the FOPID controller with higher performance accuracy can achieve smaller e_{ss}. Based on the e_{ss} values in Table 8, it shows that the MSFA-FOPID obtained the second lowest e_{ss} value after SA-FOPID with the value of 1.5467×10^{-5}, followed by the SFA-FOPID, CAS-FOPID, PSO-FOPID, and NSGA II-FOPID. However, the e_{ss} of the SCA-FOPID is unavailable to be compared as it is not reported by the author in [37]. Subsequently, the FOD, which is also the objective function of this study, represents the overall performance evaluation of the FOPID controllers based on the obtained results of M_p, t_s, t_r, and e_{ss} as shown in (6). Based on the findings from the results of M_p, t_s, t_r, and e_{ss}, it justified that the proposed MSFA-FOPID produced the best FOD than the other FOPID based methods. Specifically, the FOD attained by the MSFA-FOPID controller is 2.00, 1.79, 2.63, 1.53, 5.78, 28.56 times smaller than the SFA-FOPID, SCA-FOPID, SA-FOPID, CAS-FOPID, PSO-FOPID, and NSGA II-FOPID controllers, respectively. As a result, the MSFA-FOPID is the best controller in terms of overall performance, whereby the performance in terms of M_p, t_s, t_r, and e_{ss} are well-balanced. In addition, the NFE is introduced in this paper to highlight the advantage of the MSFA based method in term of the computational load. Generally, an optimization based method with lesser NFE indicates the method has higher computational efficiency. The NFE required by the MSFA based method in obtaining optimum FOPID controller's parameters is same as of SFA-FOPID, while 6.67, 26.67, 8.00, 8.00, and 13.33 times lesser than the SCA-FOPID, SA-FOPID, CAS-FOPID, PSO-FOPID, and NSGA II-FOPID based methods, respectively. It shows that the proposed MSFA based method has the highest computational efficiency, whereby lesser NFE is acquired to obtain optimum parameters of FOPID controller. Since the proposed MSFA based method is able to achieve the smallest FOD by requiring only 750 NFE, hence we can say that the MSFA-FOPID is the best performer.

Furthermore, in order to emphasize the improvement of the MSFA based method as compared to the standard SFA based method, the statistical analysis of the FOD in terms of best, mean, worst and standard deviations after 30 trials are presented in Table 6. The FOD obtained by the MSFA based method in terms of mean, best, worst, and standard deviation are 0.0627, 0.0209,

Table 6
The statistical analysis of the FOD in terms of best, mean, worst and standard deviations after 30 trials for SFA based FOPID controllers of AVR system.

SFA based FOPID controllers		FOD
MSFA-FOPID	Mean	0.0627
	Best	0.0209
	Worst	0.4106
	Standard deviation	0.0781
SFA-FOPID	Mean	NAN
	Best	0.0418
	Worst	NAN
	Standard deviation	NAN

Table 5
Optimized FOPID controller's parameters for AVR system.

FOPID controller	FOPID controllers' parameters				
	K_p	K_I	K_D	λ	μ
MSFA-FOPID	1.4745	0.7510	0.3700	1.0079	1.2318
SFA-FOPID	1.2605	0.9855	0.3264	1.0578	1.1615
SCA-FOPID [37]	1.4509	0.6567	0.3076	1.1442	1.2145
SA-FOPID [13]	0.7837	0.5027	0.2307	1.0103	1.0727
CAS-FOPID [34]	1.0537	0.4418	0.2510	1.0624	1.1122
PSO-FOPID [36]	1.2623	0.5531	0.2382	1.1827	1.2555
NSGA II-FOPID [35]	0.8399	1.3359	0.3512	0.9147	0.7107

Table 7
The values of P_m, ω_G, D_m, and peak gain obtained by the FOPID controllers from

FOPID controller	P_m(deg)	ω_G(rad/s)	D_m(sec)	Peak gain (dB)
MSFA-FOPID	179.8169	0.0267	117.2879	1.02×10^{-4}
SFA-FOPID	161.6158	2.4920	1.1318	0.24
SCA-FOPID [37]	176.6492	0.4667	6.6054	3.56×10^{-2}
SA-FOPID [13]	178.3847	0.1523	20.4419	1.09×10^{-3}
CAS-FOPID [34]	178.4217	0.1435	21.6890	6.62×10^{-3}
PSO-FOPID [36]	154.7012	4.3365	0.6226	7.37×10^{-2}
NSGA II-FOPID [35]	43.7524	8.3338	0.0916	4.69

Table 8
Time response specifications, FOD, and NFE of different FOPID controllers.

FOPID controller	Time response specifications				FOD	NFE
	M_p(%)	t_s(s)	t_r(s)	e_{ss}		
MSFA-FOPID	0.3628	0.1922	0.1415	1.5467×10^{-5}	0.0209	750
SFA-FOPID	3.0271	0.2304	0.1699	5.8770×10^{-3}	0.0418	750
SCA-FOPID [37]	2.4223	0.2260	0.1660	N/A	0.0374	5000
SA-FOPID [13]	0.5246	0.4057	0.2653	5.9900×10^{-7}	0.0550	20000
CAS-FOPID [34]	0.1678	0.3037	0.2223	0.0014	0.0319	6000
PSO-FOPID [36]	0.0953	0.4563	0.1375	0.0047	0.1209	6000
NSGA II-FOPID [35]	38.7887	1.2700	0.3200	1.3900×10^{-3}	0.5956	10000

0.4106, and 0.0781, respectively. Meanwhile, the FOD in terms of mean, worst, and standard deviation for the standard SFA based method are not available and only the best FOD can be obtained with the value of 0.0418. The statistical results indicate that it is difficult to guarantee the successful of the FOD's convergence in every trial due to the memoryless structure of the standard SFA based method. Therefore, according to the observation, the MSFA based method, which is augmented by the memory function in new updated formular in (12), is able to solve the unstable convergence problem and guarantee to produce better FOD in every trial consistently. Although the proposed MSFA based method requires additional objective function evaluation per iteration than the SFA based method, it is still significant to preserve a better and consistence FOD results for all 30 trials.

4.2. Bode plot analysis

The FOPID AVR systems' stability is analyzed in this subsection by analyzing the phase margin P_m, delay margin D_m and peak gain from the Bode plot. Specifically, the P_m refers to the amount of phase shift that can be handled by a system without becoming unstable, the D_m is the maximum amount of time delay that can be tolerated by the system to retain its stability, and the peak gain indicates the overshoot performance of a system. In general, a system is considered stable if the P_m is positive value while, a system with larger P_m, longer D_m, and smaller peak gain is considered to be more stable. Subsequently, the value of P_m is determined by identifying the gain crossover-frequency ω_G, where ω_G is the frequency during gain plot crosses 0 dB. Meanwhile, D_m is computed such that $D_m = (P_m/\omega_G) \times (\pi/180)$, and peak gain is the highest magnitude obtained in the gain plot.

Fig. 10 shows the Bode plot of the FOPID of AVR system tuned by MSFA, while Table 7 tabulates the values of P_m, ω_G, D_m, and peak gain of all the proposed based methods. Note that the FOPID controllers' parameters in Table 5 are used to compute the bode plot in Fig. 10. Based on the bode plot, the MSFA based method produces the most stable FOPID of AVR system, which can be indicated from the positive P_m of 179.8169°, and hereby larger than the SFA-FOPID, SCA-FOPID, SA-FOPID, CAS-FOPID, PSO-FOPID, and NSGA II-FOPID controllers by 10.12%, 1.76%, 0.79%, 0.77%, 13.96%, and 75.66%, respectively. Moreover, the MSFA-FOPID controller is also able to attain the longest D_m of 117.2879 seconds, and this is followed by the SFA-FOPID, SCA-FOPID, SA-FOPID, CAS-FOPID, PSO-FOPID, and NSGA II-FOPID controllers. Furthermore, the smallest peak gain of 1.02×10^{-4} dB is also achieved by the MSFA-FOPID controller, and come after by the SA-FOPID, CAS-FOPID, SCA-FOPID, PSO-FOPID, SFA-FOPID, and NSGA II-FOPID controllers. In overall, the proposed MSFA-FOPID controller is able to handle the largest phase shift with the smallest peak gain and also capable to tolerate the longest time delay. Thus, it justified the efficacy of the MSFA-FOPID controller for AVR system from the perspective of frequency domain analysis.

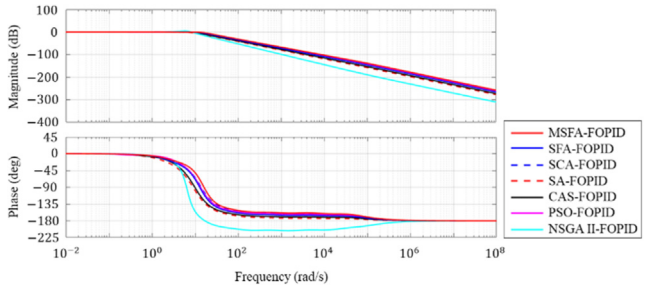

Fig. 10. Bode plot for AVR systems controlled by the FOPID controllers.

4.3. Trajectory tracking analysis

The effectiveness of the proposed MSFA-FOPID controller in trajectory tracking of reference voltage input is investigated in this section. In particular, the terminal voltage response produced by the FOPID controllers in tracking the desired trajectory is observed. Unlike the unit step input in Fig. 9, which is more uniform and predictable, the trajectory tracking analysis used the reference input voltage with combination of step and ramp as shown in Fig. 11. As a result, the ability of the controller to track the given input voltage trajectory can be more challenging since it consists of mul-

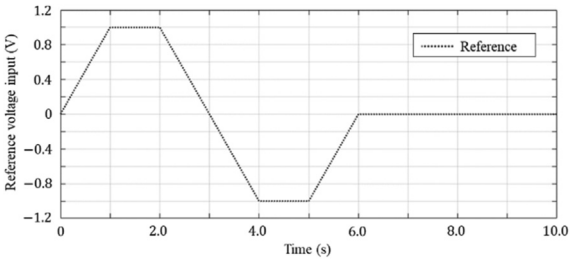

Fig. 11. The reference input signal with combination of step and ramp signals.

tiple slopes with different gradients and setpoints. Note that the same FOPID controllers tabulated in Table 5 are used in this trajectory tracking analysis. Meanwhile, the performance indicators in (13), (14), (15), and (16) are used to evaluate the effectiveness of trajectory tracking of each FOPID controller with the final simulation time of $t_f = 10.0$.

Fig. 12 shows the terminal voltage response produced by the FOPID controllers based on the given trajectory tracking input in Fig. 11. It is noticeable that the voltage response produced by the proposed MSFA-FOPID controller is slightly better than the other counterparts by tracking the reference voltage input closely throughout 10 seconds simulation time. Specifically, the zoomed-in view in the Fig. 12 reveals that the MSFA-FOPID has better trajectory tracking, where the voltage response is the closest to the reference input voltage with negligible overshoot. In the comparison of that, the NSGA II-FOPID has better accuracy along the slopes, where the voltage response is tracked closely to the reference voltage input. However, it produces the largest overshoot and unable to achieve steady state at both the positive and negative constant setpoints. Similarly, the SFA-FOPID controller produces voltage response overshoot slightly smaller than the NSGA II-FOPID controller, but still exhibits large steady error and less accuracy along the slopes. Moreover, the voltage response produced by the SCA-FOPID, SA-FOPID, CAS-FOPID, and PSO-FOPID controllers show undershoot at the positive and negative constant setpoints, which are significantly unable to track the reference input voltage. Thus, this indicates that the proposed MSFA-FOPID controller has better trajectory tracking efficacy since it produces the closest tracking of the reference input voltage.

Moreover, the performance indicators in terms of IAE, ISE, ITAE, and ITSE are recorded in Table 9 to numerically compare the effectiveness of the trajectory tracking based on the FOPID controllers. Here, the FOPID controller is considered to have good trajectory tracking control accuracy if it can exhibit minimum values of IAE, ISE, ITAE, and ITSE. As observed in Table 9, the proposed MSFA-FOPID controller outperforms its counterparts by achieving the lowest values for all indicators with the values of 0.2763, 0.0294, 0.5147, and 0.0557 for IAE, ISE, ITAE, and ITSE, respectively. Meanwhile, the PSO-FOPID controller come after as the second best FOPID controller, where the IAE, ISE, ITAE, and ITSE obtained are 0.33%, 0.29%, 0.62%, and 0.60% larger compared to the MSFA-FOPID controller, respectively. Furthermore, the SCA-FOPID controller follows up after the PSO-FOPID controller very closely as the IAE, ISE, ITAE, and ITSE obtained are highly competitive, where the values obtained are only larger by 0.01%, 0.14%, 0.01%, and 0.12% as compared to the PSO-FOPID controller, respectively. In overall, it is confirmed that the proposed MSFA-FOPID controller has significant improvement in terms of trajectory tracking efficacy compared the other existing FOPID controllers.

4.4. Disturbance rejection analysis

The robustness of the FOPID controllers is investigated in this section by observing the performance of each FOPID controller in handling the disturbance. Here, the same reference voltage input in Fig. 11 is used for the FOPID controllers to track the desired trajectory and an additional disturbance signal V_{dist} as shown in Fig. 13 is simultaneously injected into the closed-loop FOPID control of AVR system as illustrated in Fig. 14. Specifically, the disturbance signal consists of positive and negative amplitudes, which are set to $V_{dist} = 0.5$ V and $V_{dist} = -0.5$ V at simulation time $t = 3.0$ s and $t = 5.5$ s with the duration of 0.05 s, respectively. As a result, the FOPID controllers are required to track the given reference input voltage with the existence of the disturbance signal. Note that, in this analysis, the same FOPID controllers in Table 5 are employed, while the same performance indicators in (13), (14),

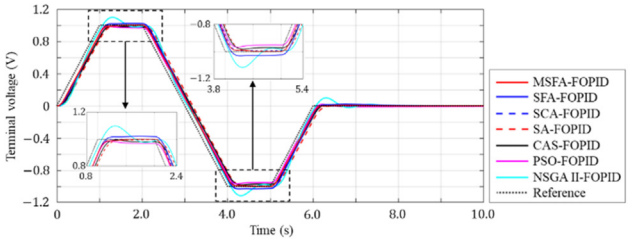

Fig. 12. Terminal voltage response with variable reference voltage input.

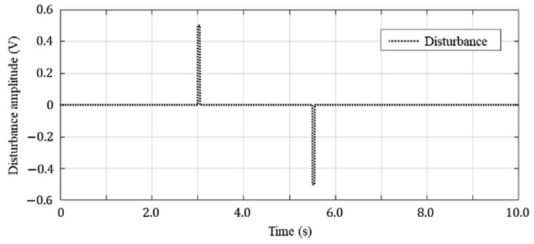

Fig. 13. The disturbance signal V_{dist}.

Table 9
The IAE, ISE, ITAE, and ITSE obtained by various FOPID controllers in terms of trajectory tracking efficacy.

FOPID controller	Performance indicator			
	IAE	ISE	ITAE	ITSE
MSFA-FOPID	0.1351	0.0762	0.0645	0.0040
SFA-FOPID	0.1720	0.0929	0.1001	0.0062
SCA-FOPID [37]	0.1558	0.0871	0.1689	0.0054
SA-FOPID [13]	0.1967	0.1328	0.0392	0.0114
CAS-FOPID [34]	0.2182	0.1172	0.1566	0.0098
PSO-FOPID [36]	0.2403	0.0885	0.4521	0.0104
NSGA II-FOPID [35]	0.4232	0.2105	0.2543	0.0476

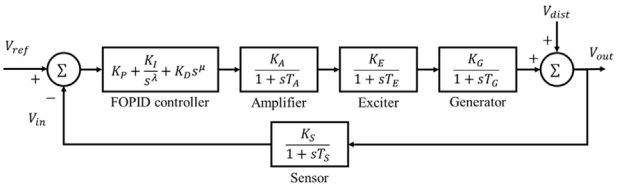

Fig. 14. The disrupted FOPID AVR system by the disturbance signal V_{dist}.

(15), and (16) are also used to evaluate the disturbance rejection efficacy.

The trajectory tracking response produced by the FOPID controllers after disrupted by the disturbance signal is illustrated in Fig. 15. It is noticed that most of the FOPID controllers are able to recover the desired trajectory after several disturbances are injected into the AVR system. Specifically, the overall trajectory tracking responses produced by the FOPID controller are similar to Fig. 12, except for the disruption at $t = 3.0$ s and $t = 5.5$ s, which are caused by the disturbance signal $V_{dist} = 0.5$ V and $V_{dist} = -0.5$ V, respectively. In order to understand more about those disruptions, the zoomed-in view for $V_{dist} = 0.5$ V and $V_{dist} = -0.5$ V are provided in Fig. 16 and Fig. 17 for detail investigation, respectively. In particular, the proposed MSFA-FOPID controller has the fastest rate of recovery while retaining smaller disruption impact than most of the counterparts, which can be seen in the zoomed-in view in Fig. 16 and Fig. 17. In the comparison of that, the disruption produced by the NSGA II-FOPID controller at $t = 3.0$ s is the lowest as observed in Fig. 16. This is because the trajectory tracking of the NSGA II-FOPID controller before the first disturbance signal is the closest to reference voltage input. However, it takes longer duration to recover from the disruption and produces large oscillation during the recovery. On the other hand, as observed in Fig. 17, the PSO-FOPID controller produces the smallest disruption impact at the second disturbance signal at $t = 5.5$ s. Nevertheless, it produces the largest overshoot after the second disturbance signal in an attempt to recover the desired reference voltage input. Furthermore, the SFA-FOPID, SCA-FOPID, SA-FOPID, and CAS-FOPID controllers produce larger disruption impact than the proposed MSFA-FOPID controller for both $V_{dist} = 0.5$ V and $V_{dist} = -0.5$ V. In overall, the proposed MSFA-FOPID controller is noticed to be superior to the other counterparts in terms of disturbance rejection since it is more robust to the disturbance signal with faster rate of recovery and produce minor overshoot in its attempt to recover the trajectory tracking.

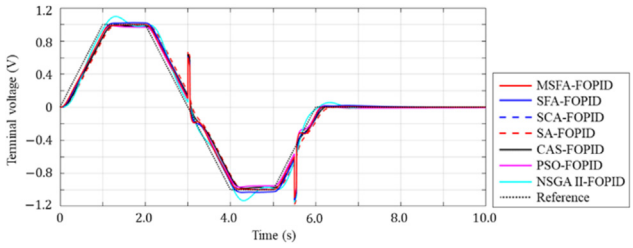

Fig. 15. The overview of trajectory tracking produced by FOPID controllers under disruption of disturbance signal.

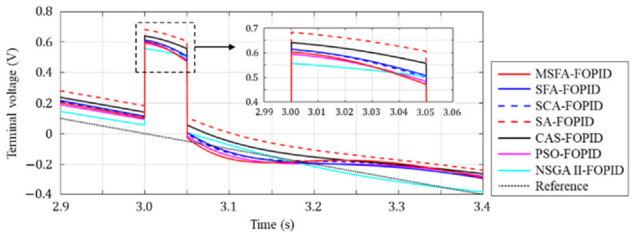

Fig. 16. The zoomed-in view of disrupt impact by $V_{dist} = 0.5$ V.

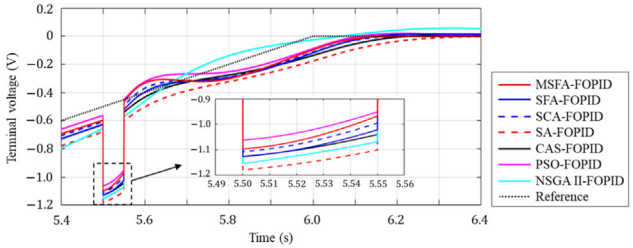

Fig. 17. The zoomed-in view of disrupt impact by $V_{dist} = -0.5$ V.

Furthermore, the numerical results in terms of IAE, ISE, ITAE, and ITSE in the existence of disturbances obtained by the FOPID controllers are recorded in Table 10. Note that the resultant values are very close to Table 9, where the proposed MSFA-FOPID controller still outperforms other FOPID controllers by obtaining the smallest values of IAE, ISE, ITAE, and ITSE, which are recorded as 0.2835, 0.0411, 0.5345, and 0.0909, respectively. Similarly, the second-best controller remained by the PSO-FOPID controller, where the attained IAE, ISE, ITAE, and ITSE values are larger by 31.53%, 21.12%, 58.62%, and 36.30% as compared to the proposed MSFA-FOPID, respectively. Then, the SCA-FOPID comes after very competitively to the PSO-FOPID controller since the IAE, ISE, and ITSE values obtained are 0.08%, 10.44%, and 0.08% larger than PSO-FOPID controller, respectively. Meanwhile, the SCA-FOPID controller has a minor improvement over the PSO-FOPID controller in terms of ITAE, as the resulting value was slightly smaller than the PSO-FOPID controller by 0.06%. Based on the above justifications and analyses, it is confirmed that the proposed MSFA-FOPID controller outperforms the other existing FOPID controllers in terms of disturbance rejection efficacy by having the most significant trajectory tracking improvement.

4.5. Parameter variation analysis

The ability of FOPID controller parameters in Table 5 to withstand with parameter variation of AVR system is evaluated in this section. In particular, the parameters of the amplifier T_A, exciter T_E, generator T_G, and sensor T_S are considered to be uncertain with the values ranging from −25% to

25% and −50% to 50% of their nominal values. Note that, since this analysis was conducted by using unit step input, the time response specification analysis in terms of steady state error, overshoot, rise time and settling time is again observed. As a result, there are a total of 64 time response specifications acquired from all of the parameter variations of T_A, T_E, T_G, and T_S as recorded in Table 11, Table 12, Table 13, and Table 14 respectively. As expected, the time response specifications performance shows larger degradation for parameter variation of −50% to 50% than −25% to 25% of their nominal values. In overall, it is shown that the proposed MSFA-FOPID controller is able to provide robust control performance and able to maintain better time response specification in most of the parameter variation cases as compared to other FOPID controllers. Specifically, the MSFA-FOPID controller provides the best results in 44 out of 64 time response specifications, which is significantly dominated up to 68.75% of the total specifications. Meanwhile, the other existing FOPID controllers specifically the SA-FOPID, PSO-FOPID, SCA-FOPID, SFA-FOPID, and CAS-FOPID are only able to provide the best results in 9, 5, 4, 1, and 1 out of 64

Table 10
The IAE, ISE, ITAE, and ITSE obtained by various FOPID controllers in the existence of disturbances.

FOPID controller	Performance indicator			
	IAE	ISE	ITAE	ITSE
MSFA-FOPID	0.3187	0.1686	0.8677	0.4023
SFA-FOPID	0.3612	0.1859	0.9265	0.4069
SCA-FOPID [37]	0.3370	0.1789	0.9594	0.4009
SA-FOPID [13]	0.3881	0.2228	0.8808	0.3991
CAS-FOPID [34]	0.4097	0.2087	1.0024	0.4045
PSO-FOPID [36]	0.4229	0.1820	1.2558	0.4139
NSGA II-FOPID [35]	0.7419	0.3182	1.7438	0.5196

Table 11
The time response specifications provided by various FOPID controllers when T_A is varied.

Controller	T_A (ROC $= +50\%$, $T_A = 0.15$)			
	$M_p(\%)$	$t_s(\mathrm{s})\ \pm 5\%$	$t_r(\mathrm{s})\ 0.1 \rightarrow 0.9$	$e_{ss}\ (\times 10^{-3})$
MSFA-FOPID	5.7623	0.3622	0.1631	0.0018
SFA-FOPID	9.9812	0.5587	0.1897	0.5856
SCA-FOPID [37]	7.9168	0.5041	0.1873	2.2133
SA-FOPID [13]	7.0508	0.6949	0.2768	0.2392
CAS-FOPID [34]	10.5429	0.6724	0.2364	1.6208
PSO-FOPID [36]	10.4868	0.5013	0.1786	9.8621
NSGA II-FOPID [35]	53.7512	2.4645	0.2190	0.7294
	T_A (ROC $= +25\%$, $T_A = 0.125$)			
	$M_p(\%)$	$t_s(\mathrm{s})\ \pm 5\%$	$t_r(\mathrm{s})\ 0.1 \rightarrow 0.9$	$e_{ss}\ (\times 10^{-3})$
MSFA-FOPID	3.2775	0.2052	0.1524	0.0016
SFA-FOPID	6.7775	0.4458	0.1797	0.5871
SCA-FOPID [37]	4.7772	0.2383	0.1773	2.2221
SA-FOPID [13]	3.9437	0.3671	0.2693	0.2396
CAS-FOPID [34]	7.2567	0.5741	0.2275	1.6211
PSO-FOPID [36]	7.3838	0.4185	0.1687	9.8525
NSGA II-FOPID [35]	48.6976	1.8549	0.2107	0.7359
	T_A (ROC $= -25\%$, $T_A = 0.075$)			
	$M_p(\%)$	$t_s(\mathrm{s})\ \pm 5\%$	$t_r(\mathrm{s})\ 0.1 \rightarrow 0.9$	$e_{ss}\ (\times 10^{-3})$
MSFA-FOPID	0.2717	0.4654	0.1313	0.0013
SFA-FOPID	2.3343	0.2252	0.1622	0.5903
SCA-FOPID [37]	0.1858	0.2300	0.1610	2.2397
SA-FOPID [13]	0.0017	0.3988	0.2717	0.2403
CAS-FOPID [34]	0.0021	0.3025	0.2179	1.6217
PSO-FOPID [36]	0	0.2067	0.1505	9.8333
NSGA II-FOPID [35]	35.7478	1.1473	0.1943	0.7392
	T_A (ROC $= -50\%$, $T_A = 0.05$)			
	$M_p(\%)$	$t_s(\mathrm{s})\ \pm 5\%$	$t_r(\mathrm{s})\ 0.1 \rightarrow 0.9$	$e_{ss}\ (\times 10^{-3})$
MSFA-FOPID	0.1962	0.4657	0.1295	0.0012
SFA-FOPID	2.2260	0.4129	0.1681	0.5919
SCA-FOPID [37]	0.1844	0.4284	0.1781	2.2486
SA-FOPID [13]	0.0017	0.5510	0.3173	0.2406
CAS-FOPID [34]	0.0019	0.4016	0.2381	1.6219
PSO-FOPID [36]	0	0.4292	0.1524	9.8236
NSGA II-FOPID [35]	27.5943	0.7548	0.1885	0.7411

Table 12
The time response specifications provided by various FOPID controllers when T_E is varied.

Controller	T_E (ROC $= +50\%$, $T_E = 0.60$)			
	$M_p(\%)$	$t_s(\text{s}) \pm 5\%$	$t_r(\text{s})\, 0.1 \rightarrow 0.9$	$e_{ss}\ (\times 10^{-3})$
MSFA-FOPID	3.2296	0.3096	0.2022	0.0029
SFA-FOPID	6.6149	0.9885	0.2306	0.5755
SCA-FOPID [37]	4.9498	0.3096	0.2304	2.1564
SA-FOPID [13]	5.9566	0.9885	0.3412	0.2374
CAS-FOPID [34]	7.4569	0.8378	0.2867	1.6246
PSO-FOPID [36]	5.2479	0.5063	0.2154	9.9585
NSGA II-FOPID [35]	46.8567	2.1607	0.2454	0.7207
	T_E (ROC $= +25\%$, $T_E = 0.50$)			
	$M_p(\%)$	$t_s(\text{s}) \pm 5\%$	$t_r(\text{s})\, 0.1 \rightarrow 0.9$	$e_{ss}\ (\times 10^{-3})$
MSFA-FOPID	1.6447	0.2351	0.1718	0.0022
SFA-FOPID	4.1913	0.2717	0.2010	0.5821
SCA-FOPID [37]	2.2732	0.2705	0.2000	2.1937
SA-FOPID [13]	3.1917	0.4148	0.3050	0.2387
CAS-FOPID [34]	5.3935	0.5994	0.2548	1.6233
PSO-FOPID [36]	4.1395	0.2525	0.1878	9.9010
NSGA II-FOPID [35]	44.9598	1.9267	0.2247	0.7293
	T_E (ROC $= -25\%$, $T_E = 0.30$)			
	$M_p(\%)$	$t_s(\text{s}) \pm 5\%$	$t_r(\text{s})\, 0.1 \rightarrow 0.9$	$e_{ss}\ (\times 10^{-3})$
MSFA-FOPID	2.4364	0.5005	0.1116	0.0079
SFA-FOPID	3.3172	0.4793	0.1374	0.5954
SCA-FOPID [37]	1.4089	0.4880	0.1343	2.2680
SA-FOPID [13]	0.0015	0.6921	0.2213	0.2410
CAS-FOPID [34]	1.9847	0.2494	0.1825	1.6189
PSO-FOPID [36]	4.1357	0.5731	0.1286	9.7844
NSGA II-FOPID [35]	40.0440	1.4318	0.1775	0.7455
	T_E (ROC $= -50\%$, $T_E = 0.20$)			
	$M_p(\%)$	$t_s(\text{s}) \pm 5\%$	$t_r(\text{s})\, 0.1 \rightarrow 0.9$	$e_{ss}\ (\times 10^{-3})$
MSFA-FOPID	6.0332	0.5419	0.0818	0.0039
SFA-FOPID	4.9026	0.5046	0.1034	0.6021
SCA-FOPID [37]	3.1601	0.5068	0.0996	2.3050
SA-FOPID [13]	0.0012	0.7940	0.1723	0.2420
CAS-FOPID [34]	1.1865	0.7037	0.1412	1.6156
PSO-FOPID [36]	5.7172	0.8659	0.0967	9.7253
NSGA II-FOPID [35]	36.1452	1.1521	0.1493	0.7536

Table 13
The time response specifications provided by various FOPID controllers when T_G is varied.

Controller	T_G (ROC $= +50\%, T_G = 1.50$)			
	$M_p(\%)$	$t_s(\text{s}) \pm 5\%$	$t_r(\text{s}) 0.1 \rightarrow 0.9$	$e_{ss}(\times 10^{-3})$
MSFA-FOPID	3.0631	0.3405	0.2262	0.0077
SFA-FOPID	6.3946	1.4437	0.2536	0.5511
SCA-FOPID [37]	3.5376	0.3526	0.2557	2.0359
SA-FOPID [13]	3.7531	0.5281	0.3866	0.2420
CAS-FOPID [34]	3.5720	0.4290	0.3174	1.6900
PSO-FOPID [36]	1.3900	0.3198	0.2353	10.3885
NSGA II-FOPID [35]	39.8388	1.5759	0.2573	0.6879
	T_G (ROC $= +25\%, T_G = 1.25$)			
	$M_p(\%)$	$t_s(\text{s}) \pm 5\%$	$t_r(\text{s}) 0.1 \rightarrow 0.9$	$e_{ss}(\times 10^{-3})$
MSFA-FOPID	1.6930	0.2540	0.1807	0.0047
SFA-FOPID	4.4299	0.2875	0.2110	0.5698
SCA-FOPID [37]	1.8678	0.2893	0.2108	2.1352
SA-FOPID [13]	1.6306	0.4502	0.3268	0.2423
CAS-FOPID [34]	3.0081	0.3648	0.2690	1.6591
PSO-FOPID [36]	1.8510	0.2658	0.1963	10.1149
NSGA II-FOPID [35]	40.9951	1.4278	0.2306	0.7126
	T_G (ROC $= -25\%, T_G = 0.75$)			
	$M_p(\%)$	$t_s(\text{s}) \pm 5\%$	$t_r(\text{s}) 0.1 \rightarrow 0.9$	$e_{ss}(\times 10^{-3})$
MSFA-FOPID	5.2604	0.4786	0.1072	0.0018
SFA-FOPID	6.5214	0.2989	0.1312	0.6078
SCA-FOPID [37]	4.4434	0.1723	0.1279	2.3230

Table 13 (*continued*)

Controller	T_G (ROC $= +50\%, T_G = 1.50$)			
	$M_p(\%)$	$t_s(s) \pm 5\%$	$t_r(s) 0.1 \rightarrow 0.9$	$e_{ss}(\times 10^{-3})$
SA-FOPID [13]	1.9392	0.2806	0.2046	0.2347
CAS-FOPID [34]	5.5091	0.3702	0.1719	1.5774
PSO-FOPID [36]	7.2432	0.5516	0.1232	9.5723
NSGA II-FOPID [35]	45.4442	1.4676	0.1719	0.7624
	T_G (ROC $= -50\%, T_G = 0.50$)			
	$M_p(\%)$	$t_s(s) \pm 5\%$	$t_r(s) 0.1 \rightarrow 0.9$	$e_{ss}(\times 10^{-3})$
MSFA-FOPID	13.0373	0.4236	0.0758	0.0053
SFA-FOPID	12.8291	0.4828	0.0943	0.6270
SCA-FOPID [37]	10.6405	0.4656	0.0906	2.4115
SA-FOPID [13]	6.0051	0.7602	0.1462	0.2264
CAS-FOPID [34]	9.9421	0.6687	0.1245	1.5274
PSO-FOPID [36]	13.3783	1.1955	0.0887	9.3030
NSGA II-FOPID [35]	49.5182	1.5047	0.1381	0.7876

Table 14
The time response specifications provided by various FOPID controllers when T_S is varied.

Controller	T_S (ROC $= +50\%, T_S = 0.0150$)			
	$M_p(\%)$	$t_s(s) \pm 5\%$	$t_r(s) 0.1 \rightarrow 0.9$	$e_{ss}(\times 10^{-3})$
MSFA-FOPID	2.5385	0.4663	0.1342	0.0015
SFA-FOPID	4.7377	0.2206	0.1631	0.5881
SCA-FOPID [37]	2.7532	0.2160	0.1600	2.2275
SA-FOPID [13]	1.3474	0.3518	0.2565	0.2398
CAS-FOPID [34]	4.6687	0.2887	0.2129	1.6211
PSO-FOPID [36]	5.5947	0.3314	0.1523	9.8449
NSGA II-FOPID [35]	45.2277	1.7188	0.2000	0.7366
	T_S (ROC $= +25\%, T_S = 0.0125$)			
	$M_p(\%)$	$t_s(s) \pm 5\%$	$t_r(s) 0.1 \rightarrow 0.9$	$e_{ss}(\times 10^{-3})$
MSFA-FOPID	1.3973	0.4496	0.1376	0.0015
SFA-FOPID	3.8489	0.2253	0.1664	0.5884
SCA-FOPID [37]	1.8923	0.2215	0.16380	2.2292
SA-FOPID [13]	0.8958	0.3584	0.2608	0.2398
CAS-FOPID [34]	4.0416	0.2937	0.2165	1.6212
PSO-FOPID [36]	4.6054	0.2094	0.1554	9.8439
NSGA II-FOPID [35]	43.9846	1.7035	0.2011	0.7370
	T_S (ROC $= -25\%, T_S = 0.0075$)			
	$M_p(\%)$	$t_s(s) \pm 5\%$	$t_r(s) 0.1 \rightarrow 0.9$	$e_{ss}(\times 10^{-3})$
MSFA-FOPID	0.3573	0.1991	0.1457	0.0015
SFA-FOPID	2.4924	0.2360	0.1738	0.5890
SCA-FOPID [37]	0.4083	0.2344	0.1722	2.2326
SA-FOPID [13]	0.1088	0.3729	0.2700	0.2400
CAS-FOPID [34]	2.9187	0.3045	0.2241	1.6216
PSO-FOPID [36]	2.8423	0.2195	0.1626	9.8419
NSGA II-FOPID [35]	41.5660	1.6629	0.2035	0.7377
	T_S (ROC $= -50\%, T_S = 0.0050$)			
	$M_p(\%)$	$t_s(s) \pm 5\%$	$t_r(s) 0.1 \rightarrow 0.9$	$e_{ss}(\times 10^{-3})$
MSFA-FOPID	0.3518	0.2070	0.1504	0.0014
SFA-FOPID	2.4764	0.2420	0.1779	0.5893
SCA-FOPID [37]	0.1870	0.2418	0.1768	2.2343
SA-FOPID [13]	0.0018	0.3808	0.2749	0.2401
CAS-FOPID [34]	2.4233	0.3104	0.2282	1.6218
PSO-FOPID [36]	2.0754	0.2253	0.1666	9.8409
NSGA II-FOPID [35]	40.3944	1.6303	0.2048	0.7381

time response specifications, respectively. Thus, the findings once again demonstrated that the proposed MSFA-FOPID controller has the highest ability to retain a good controller performance even when parameter variations arise.

5. Conclusion

In this study, a new MSFA-FOPID controller is presented to improve the regulating performance of AVR system. In particular, the purpose of this study had resulted in two findings. Firstly, the new MSFA based method had successfully developed by implementing a memorizable function in the standard SFA based method. As a result, the new MSFA based method had solved the unstable convergence of the standard SFA based method, such that the new MSFA based method is able to provide stable output and high convergence accuracy during optimization process. Secondly, the computational load to obtain the optimum FOPID controller by using MSFA is significantly lower, where only 750 NFEs are

required. This is because the MSFA based method only requires three NFEs in every iteration. Eventually, the results obtained in step response analysis has shown that the MSFA-FOPID controller is the most efficient while remain highly competitive to the other counterparts. Meanwhile, the statistical analysis also reveals that the inconsistency problem in the SFA based method has been solved by the implementation of memorizable function in the new MSFA based method. Furthermore, the MSFA-FOPID controller is the more stable than the other counterparts in the Bode plot analysis by having the ability to handle the largest phase shift with the smallest peak gain and also capable to tolerate the longest time delay. Moreover, the robustness analysis in terms of trajectory tracking, disturbance rejection, and parameter variation reveals that the MSFA-FOPID has the highest robustness by dominating in most of the IAE, ISE, ITAE, and ITSE obtained.

In overall, the obtained results indicated that the proposed MSFA-FOPID controller is highly effective and robust for terminal voltage control in AVR system. Furthermore, the MSFA based method is efficient for wide range of applications in engineering problem. Specifically, the MSFA based method has low computation load because it only requires three number of function evaluations in every iteration that is significantly less as compared to the typical multi-agent optimization methods. Therefore, the MSFA is suitable for applications in almost all low-range to high-range computational devices. Additionally, the memorizable function in the MSFA also improves the convergence accuracy has further increased the convergence efficacy. As a result, the MSFA based method's computation time has been significantly reduced thanks to the low computing load and memorizable function. For future work, the performance of the proposed MSFA-FOPID controller can be further upgraded by introducing fractional filter in the FOPID controller that consists of seven control parameters in total, specifically for solving actual engineering problem that consists of time delay. Hence, a class of FOPID controller with fractional filter can be acquired with better practical control performance.

Declaration of Competing Interest

The authors declare that they have no known competing financial interests or personal relationships that could have appeared to influence the work reported in this paper.

Acknowledgments

The highest gratitude is especially extended to the Universiti Malaysia Pahang for the financial assistance provided under Distinguished Research Grant RDU223011. Heartfelt appreciation is also further directed to University Malaysia Pahang for the monetary and resource assurances under its postgraduate research scheme (PGRS) (PGRS200350).

References

[1] R.K. Tripathi, C.P. Singh, Power quality control of unregulated non-linear loads, in: *ICPCES 2010 - International Conference on Power, Control and Embedded Systems*, 2010, https://doi.org/10.1109/ICPCES.2010.5698627.
[2] P.K. Mohanty, B.K. Sahu, S. Panda, Tuning and assessment of proportional-integral-derivative controller for an automatic voltage regulator system employing local unimodal sampling algorithm, Electric Power Comp. Syst. 42 (9) (2014), https://doi.org/10.1080/15325008.2014.903546.
[3] A.H. Mary, A.H. Miry, M.H. Miry, An optimal robust state feedback controller for the AVR system-based harris hawks optimization algorithm, Electric Power Comp. Syst. 48 (16–17) (2021), https://doi.org/10.1080/15325008.2021.1908456.
[4] N. Pachauri, Water Cycle Algorithm-Based PID Controller for AVR, COMPEL – Int. J. Comput. Mathem. Electr. Electr. Eng. 39 (3) (2020), https://doi.org/10.1108/COMPEL-01-2020-0057.
[5] O. Bendjeghaba, Continuous firefly algorithm for optimal tuning of PID controller in AVR system, J. Electr. Eng. 65 (1) (2014), https://doi.org/10.2478/jee-2014-0006.
[6] G. Zhou, J. Li, Z. Tang, Q. Luo, Y. Zhou, An improved spotted hyena optimizer for PID parameters in an AVR system, Mathem. Biosci. Eng. 17 (4) (2020), https://doi.org/10.3934/MBE.2020211.
[7] S. Veinović, D. Stojić, D. Joksimović, Optimized four-parameter PID controller for AVR systems with respect to robustness, Int. J. Electr. Power Energy Syst. 135 (2022), https://doi.org/10.1016/j.ijepes.2021.107529.
[8] E. Kose, Optimal control of AVR system with tree seed algorithm-based PID controller, IEEE Access 8 (2020), https://doi.org/10.1109/ACCESS.2020.2993628.
[9] A.J.H. Al Gizi, M.W. Mustafa, N.A. Al-geelani, M.A. Alsaedi, Sugeno fuzzy PID tuning, by genetic-neutral for AVR in electrical power generation, Appl. Soft Comput. J. 28 (2015), https://doi.org/10.1016/j.asoc.2014.10.046.
[10] S. Ekinci, B. Hekimoglu, Improved kidney-inspired algorithm approach for tuning of PID controller in AVR system, IEEE Access 7 (2019), https://doi.org/10.1109/ACCESS.2019.2906980.
[11] Z.L. Gaing, A particle swarm optimization approach for optimum design of PID controller in AVR system, IEEE Trans. Energy Convers. 19 (2) (2004), https://doi.org/10.1109/TEC.2003.821821.
[12] V.K. Bhatt, S. Bhongade, Design of PID controller in automatic voltage regulator (AVR) system using PSO technique, Int. J. Eng. Res. Appl. (IJERA) 3 (4) (2013).
[13] R. Lahcene, S. Abdeldjalil, K. Aissa, Optimal Tuning of Fractional Order PID Controller for AVR System Using Simulated Annealing Optimization Algorithm. In *2017 5th International Conference on Electrical Engineering - Boumerdes, ICEE-B 2017*; 2017; Vol. 2017-January. 10.1109/ICEE-B.2017.8192194.
[14] Z. Bingul, O. Karahan, A novel performance criterion approach to optimum design of PID controller using cuckoo search algorithm for AVR system, J. Franklin Inst. 355 (13) (2018), https://doi.org/10.1016/j.jfranklin.2018.05.056.
[15] M. Ćalasan, M. Micev, Ž. Djurovic, H.M.A. Mageed, Artificial ecosystem-based optimization for optimal tuning of robust PID controllers in AVR systems with limited value of excitation voltage, Int. J. Electr. Eng. Educ. (2020), https://doi.org/10.1177/0020720920940605.
[16] S. Mohd Helmi, A. Mohd Ashraf, Optimal tuning of sigmoid PID controller using nonlinear sine cosine algorithm for the automatic voltage regulator system, J. ISA Trans. (2021).
[17] J. Bhookya, R.K. Jatoth, Optimal FOPID/PID controller parameters tuning for the AVR system based on sine–cosine-algorithm, Evol. Intel. 12 (4) (2019), https://doi.org/10.1007/s12065-019-00290-x.
[18] K. Gnaneshwar, R. Trivedi, P.K. Padhy, Optimal tuning of FOPID parameters with SFL algorithm for an AVR system, in: *Proceedings of the 4th International Conference on Electronics, Communication and Aerospace Technology*, 2020, https://doi.org/10.1109/ICECA49313.2020.9297551.
[19] C. Srikanth, D.G. Padhan, N.K. Kumar, Avr System analysis and simulation by using fopid and parameters variation effects, E3S Web Conf. 309 (2021), https://doi.org/10.1051/e3sconf/202130901033.
[20] S.F. Aliabadi, S.A. Taher, Design of fuzzy-FOPID controller optimized by ICA for control of AVR. *Majlesi*, J. Electr. Eng. 11 (4) (2017).
[21] A. Sikander, P. Thakur, R.C. Bansal, S. Rajasekar, A novel technique to design cuckoo search based FOPID controller for AVR in power systems, Comput. Electr. Eng. 70 (2018), https://doi.org/10.1016/j.compeleceng.2017.07.005.
[22] J. Bhookya, R.K. Jatoth, Improved jaya algorithm-based FOPID/PID for AVR system, COMPEL – Int. J. Comput. Mathem. Electr. Electr. Eng. 39 (4) (2020), https://doi.org/10.1108/COMPEL-08-2019-0319.
[23] S. Shu, Y. Zhang, X. Wang, Q. Pan, X. Tao, Space vector control of a permanent magnet linear synchronous motor based on the improved single neuron PID algorithm, Control Eng. Appl. Inf. 22 (3) (2020).
[24] Thanh, L. M.; Thuong, L. H.; Loc, P. T.; Nguyen, C. N. Delta robot control using single neuron PID algorithms based on recurrent fuzzy neural network identifiers. *Int. J. Mech. Eng. Robotics Research*, **2020**, *9* (10). 10.18178/ijmerr.9.10.1411-1418.
[25] P. Fu, J. Guo, J. Ding, G. Zhou, R. Shen, Neuron adaptive PID speed and position control for ultrasonic motors, Diangong Jishu Xuebao/Trans. China Electrot. Soc. 22 (2) (2007).
[26] [Mien, T. L.; van An, V.; Tam, B. T. A Fuzzy-PID Controller Combined with PSO Algorithm for the Resistance Furnace. *Advances in Science, Technology and Engineering Systems*, **2020**, *5* (3). 10.25046/aj050371.
[27] C.T. Chao, N. Sutarna, J.S. Chiou, C.J. Wang, An optimal fuzzy PID controller design based on conventional PID control and nonlinear factors, Appl. Sci. (Switzerland) 9 (6) (2019), https://doi.org/10.3390/app9061224.
[28] H. Maghfiroh, M. Ahmad, Ramelan, A.; Adriyanto, F. Fuzzy-PID in BLDC motor speed control using MATLAB/simulink. *J. Robotics Control (JRC)*, **2022**, *3* (1). 10.18196/jrc.v3i1.10964.
[29] A. Ates, B.B. Alagoz, Yeroglu, C.; Alisoy, H. Sigmoid Based PID Controller Implementation for Rotor Control. In *2015 European Control Conference, ECC 2015*; 2015. 10.1109/ECC.2015.7330586.
[30] N.H.A. Razak Ramesh, M.R. Ghazali, M.A. Ahmad, Sigmoid Pid Based Adaptive Safe experimentation dynamics algorithm of portable duodopa Pump for Parkinson's Disease Patients. *Bull. Electr. Eng. Inf.*, **2021**, *10* (2). 10.11591/eei.v10i2.2542.
[31] R.L.A. Ribeiro, C.M.S. Neto, F.B. Costa, T.O.A. Rocha, R.L. Barreto, A sliding-mode voltage regulator for salient pole synchronous generator, Electr. Power Syst. Res. 129 (2015), https://doi.org/10.1016/j.epsr.2015.07.016.
[32] M.S. Ayas, Design of an optimized fractional high-order differential feedback controller for an AVR system, Electr. Eng. 101 (4) (2019), https://doi.org/10.1007/s00202-019-00842-5.
[33] M.J. Mohamed, M.A. Khashan, Comparison between PID and FOPID controllers based on particle swarm optimization. In *The Second Engineering Conference of Control, Computers and Mechatronics Engineering (ECCCM2, 2014)*; 2014.

[34] Y. Tang, M. Cui, C. Hua, L. Li, Y. Yang, Optimum design of fractional order PI ΛD μ controller for AVR system using chaotic ant swarm, Expert Syst. Appl. 39 (8) (2012), https://doi.org/10.1016/j.eswa.2012.01.007.
[35] I. Pan, S. Das, Chaotic multi-objective optimization based design of fractional order PI ΛD μ controller in AVR system, Int. J. Electr. Power Energy Syst. 43 (1) (2012), https://doi.org/10.1016/j.ijepes.2012.06.034.
[36] H. Ramezanian, S. Balochian, A. Zare, Design of optimal fractional-order PID controllers using particle swarm optimization algorithm for automatic voltage regulator (AVR) system, J. Control, Automat. Electr. Syst. 24 (5) (2013) 601–611, https://doi.org/10.1007/s40313-013-0057-7.
[37] M.S. Ayas, E. Sahin, FOPID controller with fractional filter for an automatic voltage regulator, Comput. Electr. Eng. 90 (2021), https://doi.org/10.1016/j.compeleceng.2020.106895.
[38] S. Bhatnagar, V.S. Borkar, Multiscale chaotic SPSA and smoothed functional algorithms for simulation optimization, Simulation 79 (10) (2003) 568–580, https://doi.org/10.1177/0037549703039988.
[39] D. Ghoshdastidar, A. Dukkipati, S. Bhatnagar, Smoothed functional algorithms for stochastic optimization using Q-Gaussian distributions, ACM Trans. Model. Comput. Simul. (2014), https://doi.org/10.1145/2628434.
[40] H.L. Prasad, L.A. Prashanth, S. Bhatnagar, N. Desai, Adaptive smoothed functional algorithms for optimal staffing levels in service systems, Service Sci. (2013), https://doi.org/10.1287/serv.1120.0035.
[41] S. Bhatnagar, Adaptive Newton-based multivariate smoothed functional algorithms for simulation optimization, ACM Trans. Model. Comput. Simul. (2007), https://doi.org/10.1145/1315575.1315577.
[42] Y. Tanaka, S.I. Azuma, T. Sugie, Simultaneous perturbation stochastic approximation with norm-limited update vector, Asian J. Control (2015), https://doi.org/10.1002/asjc.1153.
[43] M.A. Ahmad, M.R. Hao, R.M.T.R. Ismail, A.N.K. Nasir, Model-free wind farm control based on random search, in: *2016 IEEE International Conference on Automatic Control and Intelligent Systems (I2CACIS)*, 2016, pp. 131–134.
[44] G. Schrack, M. Choit, Optimized relative step size random searches, Math. Program. 10 (1) (1976) 230–244, https://doi.org/10.1007/BF01580669.
[45] S. Chatterjee, V. Mukherjee, PID controller for automatic voltage regulator using teaching-learning based optimization technique, Int. J. Electr. Power Energy Syst. 77 (2016), https://doi.org/10.1016/j.ijepes.2015.11.010.
[46] A. Gosavi, Parametric optimization: stochastic gradients and adaptive search, in: Simulation-Based Optimization, Springer, 2015, pp. 71–122.
[47] M.A. Ahmad, S.I. Azuma, T. Sugie, Identification of continuous-time hammerstein systems by simultaneous perturbation stochastic approximation, Expert Syst. Appl. (2016), https://doi.org/10.1016/j.eswa.2015.08.041.
[48] Y.Q. Chen, I. Petráš, D. Xue, Fractional order control – A tutorial, in: *Proceedings of the American Control Conference*, 2009, https://doi.org/10.1109/ACC.2009.5160719.
[49] Z. Gao, X. Liao, Improved oustaloup approximation of fractional-order operators using adaptive chaotic particle swarm optimization, J. Syst. Eng. Electron. 23 (1) (2012), https://doi.org/10.1109/JSEE.2012.00018.
[50] D. Baleanu, A.C.J. Luo, M.J.A.T. Fractional, Dyn. Control (2012), https://doi.org/10.1007/978-1-4614-0457-6.